Analysis of Radioactive Beam Shift on Target using ^{11}Li Scattering from Ag and H_2 Targets

by Matthew Keefe

April 2016

A Thesis Submitted to Saint Mary's
University, Halifax, Nova Scotia in Partial Fulfillment
of the Requirements for the Degree of Double Honours in
Astrophysics and Chemistry.

[April, 2016], Halifax, Nova Scotia

Approved:

Approved:

Date:

Analysis of Radioactive Beam Shift on Target using ^{11}Li Scattering from Ag and H_2 Targets

by Matthew Keefe

April 2016

Abstract

Date: April 2016

The halo nucleus ^{11}Li was explored through elastic and inelastic scattering off protons at the TRIUMF facility in Vancouver using the IRIS facility. IRIS pioneers in using thin windowless solid hydrogen target to measure reactions with radioactive ion beams at low energy. To examine the excitation spectrum of ^{11}Li, the excitation energy was found from the scattering angle and energy. It is important to evaluate the effect of beam position relative to the center of the solid hydrogen target. A shift in the beam can lead to energy differences of $\sim 0.5\%$ to 1% depending on the incident angle on the detector. The focus of this thesis is to investigate the beam position on the target relative to the detectors.

1 Introduction

The research done for this thesis was done at the TRIUMF facility in Vancouver, Canada during the summers of 2013 and 2015. This work included radioactive ion beam production along with the analysis of the bound system of ^{11}Li. This thesis focusses on the beam production of various radioactive isotopes along with the ^{11}Li beam itself. During the experiment, the ^{11}Li beam was periodically collimated with a 2mm collimator to ensure the beam hit the target within 2mm of the center of the detectors. Though this was done, the beam could still move and the wouldn't necessarily hit the target at the point that corresponds to the center of the detector(s). This can be accounted for if the position of the beam relative to the detector(s) is known.

1.1 Radioactivity

Radioactivity was accidentally discovered by Antoine Henri Becquerel (a French Physicist) in 1896 by having photographic plates in the same (dark) place as uranium salts [3]. He then attempted to replicate the experiment by placing these salts, wrapped in black paper, in the same place as photographic plates. Black paper stops visible light from passing through but Becquerel found the photographic plates were once again fully exposed. These were initially called "Becquerel Rays" and were thought to have been an invisible form of phosphorescence [3].

Marie Curie and her husband Pierre Curie continued work on radiation only just after Becquerel did his work on the subject [2]. Curie coined the term radioactivity and used it to describe all materials that exhibit this phenomenon. Curie goes on to talk about "atomic transitions" of radioactive elements. The example she gives in support of this claim is the formation of chemically defined Helium starting from chemically defines Radium; a process now known as alpha decay.

1.2 Radioactive Decay

The first example of radioactive decay was found by Becquerel in 1896 though he did now know what it was. Though not mentioned in 3, it is likely the isotope of Uranium in Becquerel's work was ^{238}U and thus the type of decay is alpha decay. Another example of alpha decay was mentioned in 2 when Curie observed the decay of Radium into an alpha particle and Radon. Alpha decay can be described generally by equation 1 below.

$$ {}^{A}_{Z}X \rightarrow {}^{A-4}_{Z-2}Y + {}^{4}_{2}He \tag{1} $$

Though alpha decay was the first radioactive decay discovered, it is not the only type (or even the most common type) of decay. Discovered by Ernest Rutherford in 1899, beta decay is the process of a neutron decaying into a proton, beta particle and an anti-electron neutrino. A general example of beta decay is described by equation 2.

$$ {}^{A}_{Z}X \rightarrow {}^{A}_{Z+1}Y + \beta^{-} + \bar{\nu}_{e} \tag{2} $$

This particular example is of β^{-} decay which is just one variety of beta decay. The other type, β^{+} decay, was discovered by Frédéric and Irène Joliot-Curie in 1934 [1]. They found it to be similar to the cosmic rays detected by Carl Anderson in 1932. These cosmic rays were the first example of positron emission and a general example can be seen in equation 3. Beta-plus decay occurs when a proton decays into a neutron releasing a positron and an electron neutrino.

$$ {}^{A}_{Z}X \rightarrow {}^{A}_{Z-1}Y + \beta^{+} + \nu_e \tag{3} $$

Gamma decay, the final type of decay, occurs when an excited nucleus relaxes to a lower-energy state. This typically occurs after a reaction that excited the nucleus or some kind of decay. The work done in the summer of 2015 in yield measurements of radioactive ion beams was focussed on beta-delayed gamma decay. This is the process of a parent nucleus undergoing beta emission that results in a daughter nucleus in an excited state. The daughter particle then relaxes and emits a gamma ray (photon).

1.3 Rutherford Scattering

Rutherford and his colleagues (Geiger and Marsden) worked with alpha-source radiation and the alpha particles were shot at different types of foils. The most well known was Rutherford's gold foil experiment where he used radium as his alpha source in 1909 [5]. From these experiments, Rutherford and his colleagues noticed that some of the alpha particles got back-scattered which was impossible when following Thompson's plum-pudding model. From this, the three researchers developed an equation to describe this scattering.

$$ N(\theta) = \left(\frac{Ze^2}{4\pi\epsilon_o}\right)^2 \frac{N_i n l}{2r^2 T \sin^4\left(\frac{\theta}{2}\right)} \tag{4} $$

Where Z is atomic number, N_i is number of incident particles, n is number density, l is the thickness of the target, r is the distance from the incident particle (^{11}Li) to the target (silver), T is the kinetic energy of the particle and θ is the scattering angle. The amount that a particle scatters falls off with $\sin^4(\theta/2)$ as seen in the above equation. This can be

graphically shown as in figure 1.

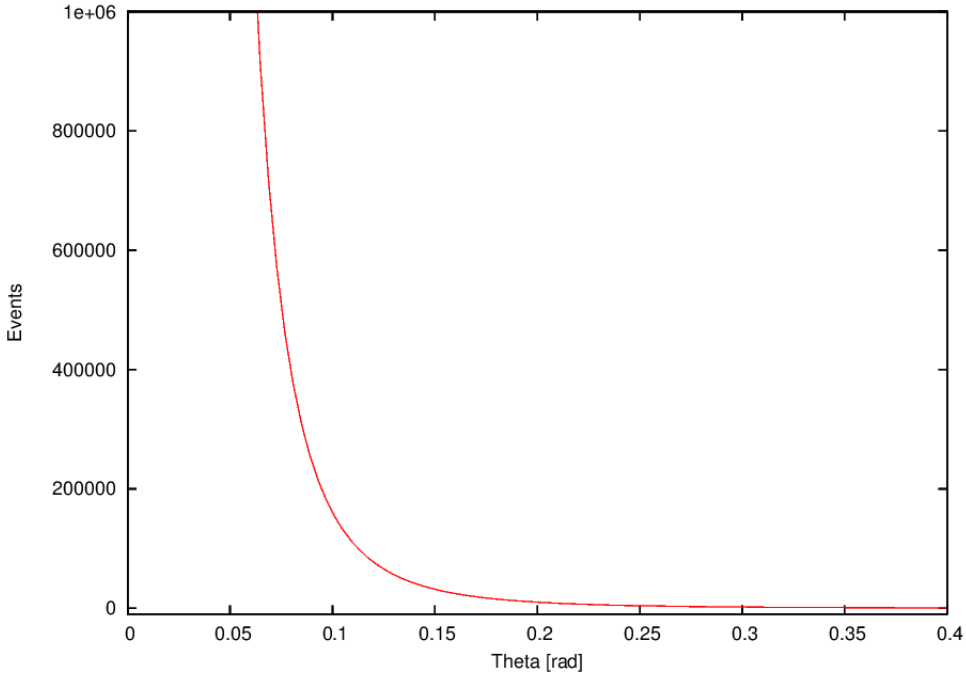

Figure 1: Relationship between number of particles and scattering angle as seen in equation 4

1.4 Halo Nuclei

When an isotope of an element is at, or close to, the neutron/proton drip line it might be possible for such isotopes to have a halo of nucleons. A halo is formed when one or two nucleons are very weakly bound to a core nucleus and have a high probability of being located far away from it. The first halo nucleus discovered was ^{11}Li [7]. This is a Borromean system with a two neutron halo and a ^{9}Li core. In such a system, if any of the three components are removed, the remaining system is unbound and breaks into its constituents. The two neutron halo such as ^{11}Li gives rise to the breakdown in the previously accepted relationship between nucleon number and root mean square radius of a nucleus (equation 5)

$$r = r_o A^{1/3} \tag{5}$$

This break of relationship can be seen in figure 2 when comparing ^{11}Li and ^{208}Pb.

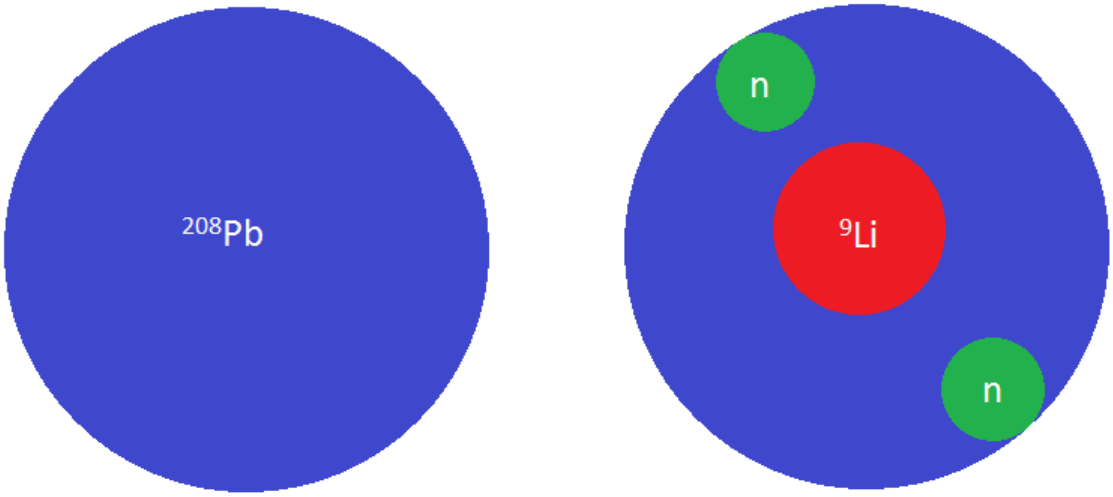

Figure 2: Comparison of the size of a light nucleus with a halo, ^{11}Li to a heavy nucleus ^{208}Pb without one.

^{11}Li is not the only halo nucleus in existence (such as ^{6}He, ^{17}B, and ^{22}C) but it was the first discovered and the nucleus of interest in this work.

2 Experiment

2.1 The IRIS Facility

Located in Vancouver, Canada, TRIUMF is Canada's National Laboratory for particle and nuclear physics. Split into two halls (ISAC-I and ISAC-II), the ISAC (**I**sotope **S**eparation and **AC**celeration) facility is used to create the **R**adioactive **I**on **B**eam (RIB) by accelerating protons and colliding them with a target (in the case of ^{11}Li , Tantalum). This reaction is a fragmentation reaction whose products are separated with a Mass Separator via the ISOL method (**I**sotope **S**eparator **O**n-**L**ine). The ^{11}Li is then post accelerated using a superconducting **LIN**ear **AC**celerator to 6A MeV which is then transported to the IRIS facility. The IRIS Facility is the **I**SAC Cha**R**ged Part**I**cles **S**pectroscopy Station. IRIS pioneers in the use of thin windowless solid Hydrogen target for studying reactions of rare isotopes. IRIS is in the ISAC-II hall and the IRIS setup is shown below in figure 3.

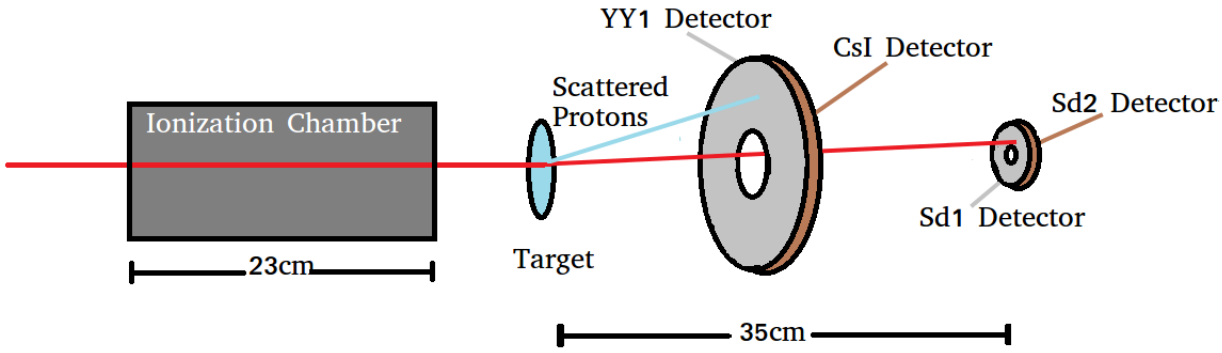

Figure 3: The setup of the IRIS facility at TRIUMF. The red line represents the beam where the blue is the scattered protons. For reference purposes, upstream is to the left of the image where downstream is to the right.

The **I**onization **C**hamber (IC), shown on the left, is filled with isobutane gas at 19.5 Torr.

The detector is used to count the beam in order to determine the incident beam intensity. The target cell has a backing of 5.44 μm of silver foil on which solid hydrogen is formed facing downstream. The first detector is a silicon strip detector array (referred to as the YY1 detector). It is separated into eight sectors and sixteen rings. The YY1 detector is used to measure the energy loss of light particles such as protons, deuterons, and tritons after the beam reacted with the H_2 target. The detector immediately behind it is the CsI detector which is an inorganic scintillator. It is used to stop the particles and measure the remaining energy after the YY1 detector. The combination of these detectors is used to obtain a **P**article **ID**entification (PID) spectrum. The PID spectrum is used to identify the type of light particle detected by energy loss and total energy correlation. This allows for identification by the charge and mass of the particles.

Downstream of the YY1 and CsI detectors are the S3 detectors (Sd1 and Sd2 in figure 3). Both of these are silicon detectors that detect the heavy particles (in this case,^{11}Li and other products). The Sd1 detector (the more upstream detector) is 60 μm thick while the Sd2 detector (placed immediately downstream) is 500 μm thick. The heavy particles can pass through the Sd1 detector, depositing part of their energy, and stop in the Sd2 detector. This allows the construction of the PID spectrum as done with the YY1 and CsI detectors for the identification of particles. The energy lost by a particle in a medium is proportional to the square of the charge of the ion. The S3 detectors, like the YY1 detector, are segmented into azimuthal sectors (thirty-two) and concentric rings (twenty-four). These detectors are unlike the YY1 detector in that they are double-sided silicon detectors with their sectors and rings are on opposite sides. The way these detectors are oriented is the sector side of the Sd1 detector is facing upstream where the sector side of the Sd2 detector is facing downstream. This causes an inversion of the sectors numbering scheme that is adapted in this report as shown in figure 4.

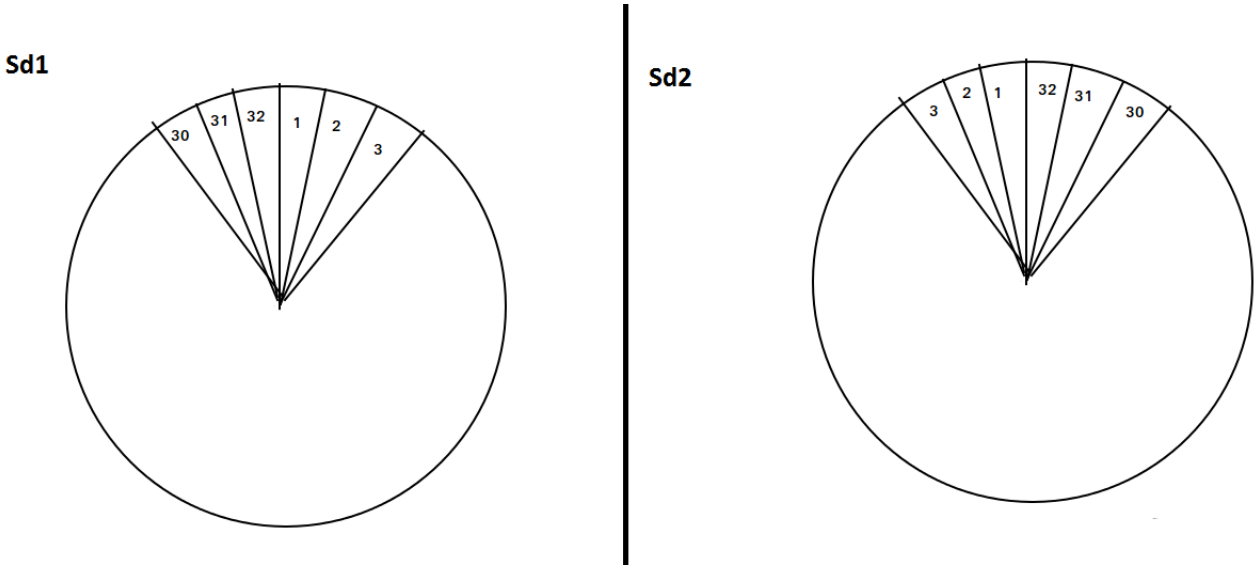

Figure 4: The orientation of the sectors in the Sd1 (left) and Sd2 (right) detectors.

2.2 Scattering

After the beam passes through the Ionization Chamber, it interacts with the target. It undergoes scattering with the silver foil via Rutherford Scattering. The scattering leads to an azimuthally symmetric distribution. After the passing through the silver foil, the beam interacts with the solid H_2 target. The scattered protons are also distributed in a symmetric way. Ideally, the beam position on the silver foil and H_2 target is centred and is aligned with the center of the detectors. This would cause the number of events to be approximately the same across all sectors in both the YY1 and the S3 detectors. This can be monitored using the hit pattern of the sectors of these detectors. The hit pattern is the amount of events recorded in a sector plotted against sector number. Due to the inversion of the sector numbering in the S3 detectors, the hit patterns will be inverted to each other and this can be seen in figure 5.

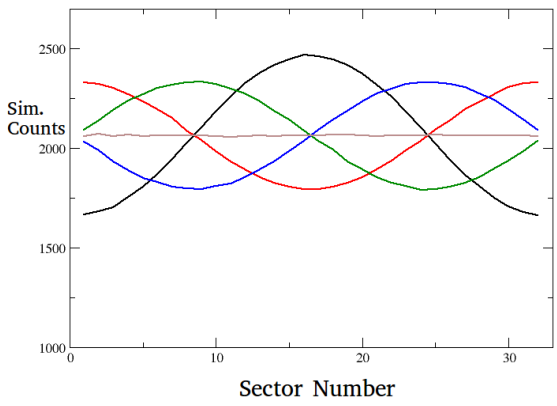

(a) Sd1 simulated hit pattern.

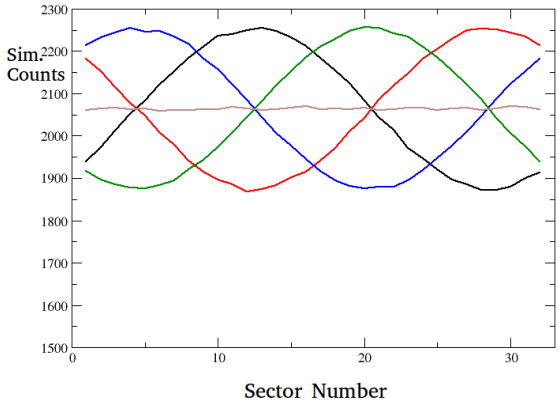

(b) Sd2 simulated hit pattern.

Figure 5: These simulations use simulated events for a particular shift. The gray line in both figures 5a 5b represents a hit pattern with no shift. The black and red curves represent a vertical shift of -2 mm and 2 mm respectively. The green and black curves represent a horizontal shift of 2 mm and -2 mm respectively. The red curve in figure 5b represents a hit pattern with vertical and horizontal shifts of 1 mm each. The black curve represents a hit pattern with a vertical and horizontal shifts of -1 mm each. The green curve represents a hit patterns with vertical and horizontal shifts of 1mm and -1mm respectively. The blue curve represents a hit patterns with vertical and horizontal shifts of -1mm and 1mm respectively.

The hit patterns of each detector can be analysed and fitted with a simulated hit pattern. A simulated hit pattern is the hit pattern for a particular shift that is produced by using a Monte Carlo method. The result of the fit will give shift of the beam. The hit patterns for the YY1 detector will appear different as there is a heat shield masking part of the detector. Because of this, only the small angles can be analysed for shifts. The orientation of the shield on the YY1 detector is given by figure 6.

The heat shield exists to protect the target cell from heating up and subliming to H_2 gas. The shield covers different amounts of each sector which means in order to get a reliable hit pattern, only the small angles can be used.

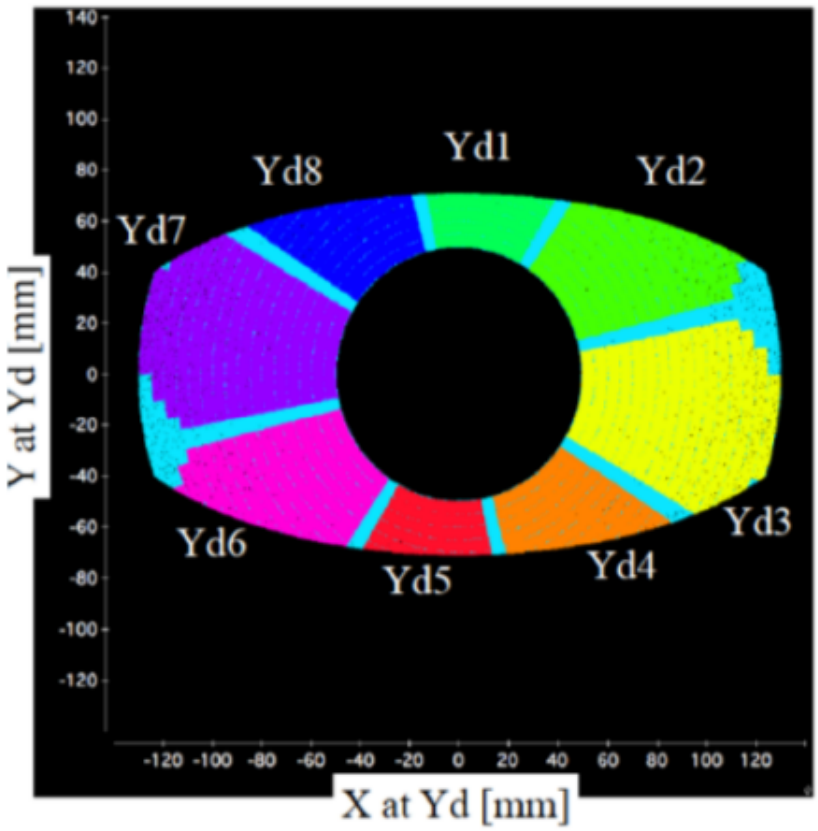

Figure 6: The coloured portions of the YY1 detector (labled Yd1-Yd8) are the sectors of the YY1 detector. The portions of the dectors that are not covered by the heat shield are seen in colour. This figure was acquired by [6].

3 Data and Analysis

3.1 Shift for S3 Detectors

In order to find the shift of the beam, the hit pattern of a detector must be examined. An example hit pattern from the Sd1 detector can be seen in figure 7. This data contains all the various reaction channels along with noise, it is not just the Ag(^{11}Li,^{11}Li)Ag reaction.

The reaction where the data for the hit patterns was acquired from the Ag(^{11}Li,^{11}Li)Ag reaction. This was accomplished by looking at a **P**article **I**dentification **S**pectra, as seen in figure 8. In order to make sure the elastic reaction was analysed, the data is first taken from the first silicon detector in the setup (YY1 in figure 3) and the CsI detector immediately

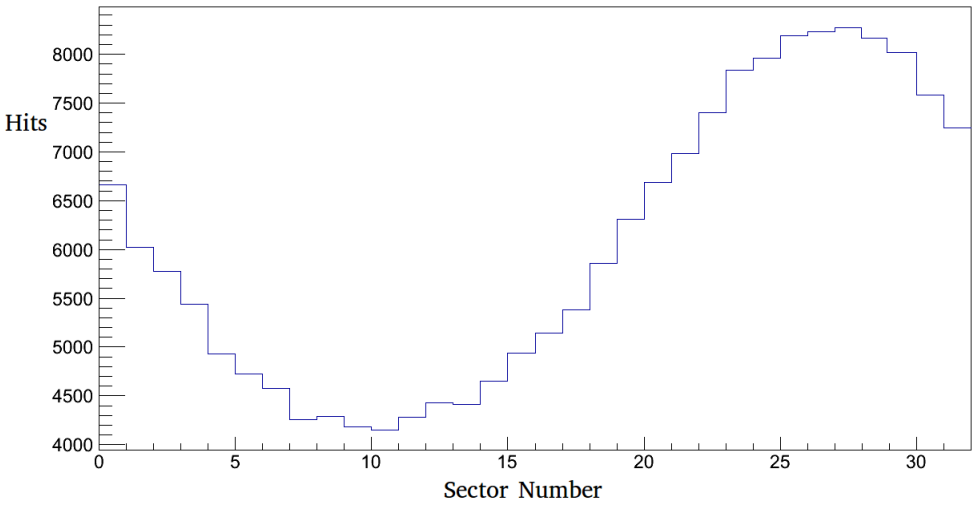

Figure 7: The hit pattern from the Sd1 detector for one of the runs done at IRIS in 2015 while finding data for the Ag(^{11}Li,^{11}Li)Ag reaction. The sector number on the horizontal axis corresponding to the sector numbers in figure 4.

behind it. The Delta-E vs E plot (PID) was created and analysed.

The gated protons are used to further the even though the protons were gated, the gate includes all protons not just the protons from the elastic reaction channel. The four loci in the above figure are protons, deuterons, tritons and higher on the plot are alpha particles. The locus that is outlined is for the protons and this is the selection process termed as "gating". This must be included to limit the reaction to just the elastic reaction. This is done using the silicon detectors downstream of the YY1 detector. The PID using the two S3 detectors can be seen in figure 9.

The elastic Ag(^{11}Li,^{11}Li)Ag reaction has now been exclusively selected to be analysed. The hit pattern containing only the desired reaction can be seen in figure 10. This selection was done for all runs using the S3 detectors for finding the hit patterns. Figure 10 is the hit pattern for the Sd1 detector and figure 11 is the hit pattern for the Sd2 detector.

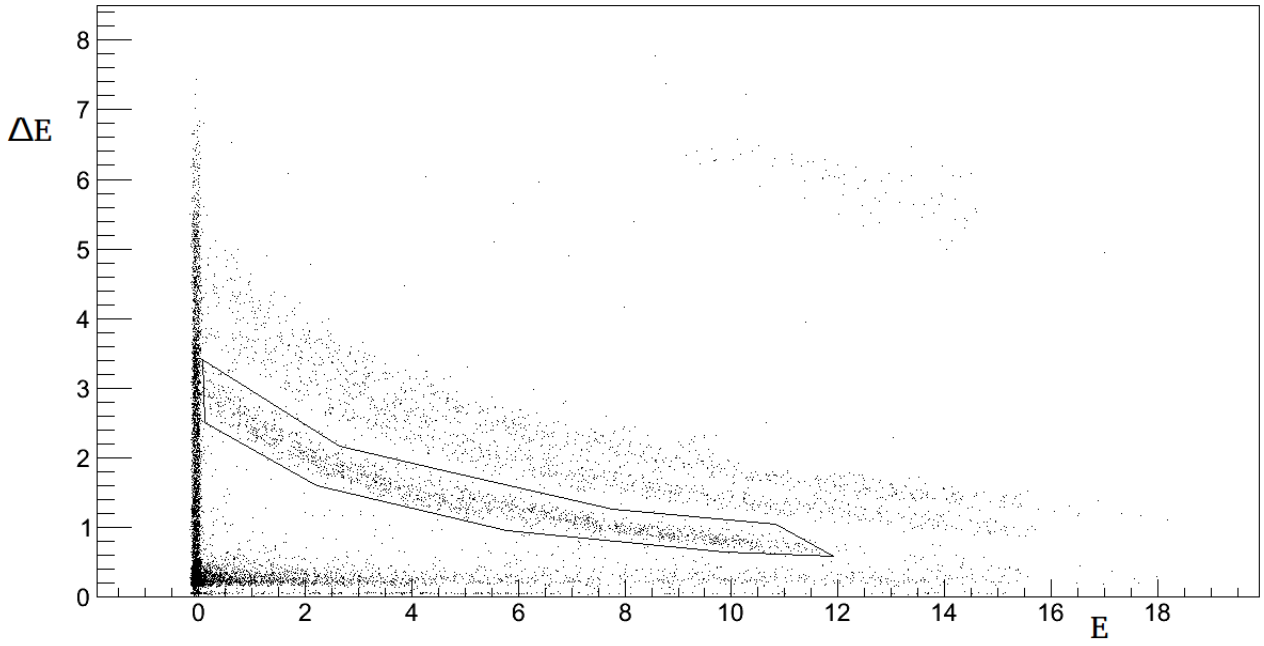

Figure 8: This is a Delta-E vs E plot from the YY1 and CsI detectors as seen in figure 3. The YY1 is thin and made of silicon so the particles will lose a small amount of energy and penetrate through to the CsI detector where they will stop and deposit all their remaining energy.The four loci in the above figure are protons, deuterons, tritons and higher on the plot are alpha particles. The locus that is outlined are the protons.

Plots such as figures 10 and 11 were created for all runs using CERN's ROOT software. A simulation code with analysis function based on C++ to model a shift. This code works by providing an initial guess value for the beam shift which it then models a hit pattern for that detector for said detector using a Monte Carlo method of integration. The χ^2 value for the shift is then calculated and the shift parameters are then reported. The code repeats this process until the χ^2 value has reached a minimum. The shifts corresponding to χ^2_{min} were plotted and can be seen in figures 12 and 13.

The shifts using the S3 detectors were found for each data run and plotted as a function of the run number to see how the beam position varied over the course of the experiment. Figures 14 and 15 show the vertical and horizontal shifts, respectively. The simulation was run multiple times, outputting a variety of shifts which the uncertainty was calculated from.

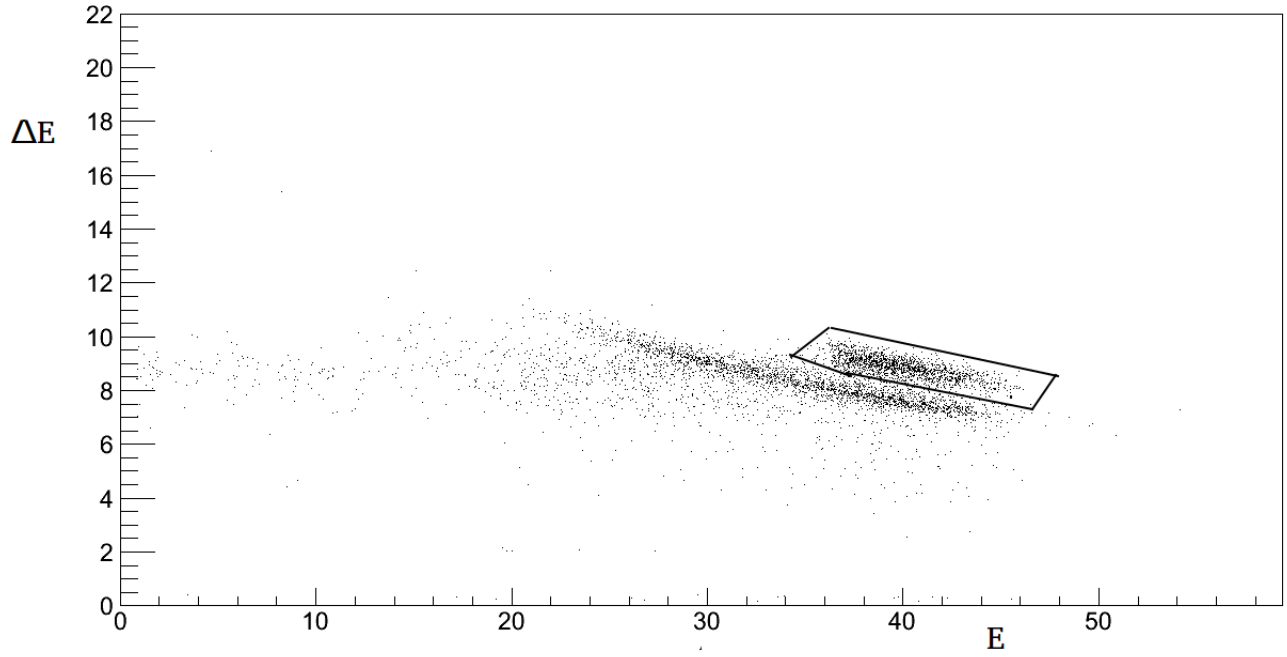

Figure 9: This is a ΔE vs E plot from the two S3 detectors. Similar to figure 8, the vertical axis is the energy deposited in the upstream detector (Sd1) and the horizontal axis is the remaining energy of the particle (deposited in the downstream, Sd2, detector). The gated locus are the ^{11}Li particles and the locus below it are the ^{9}Li particles.

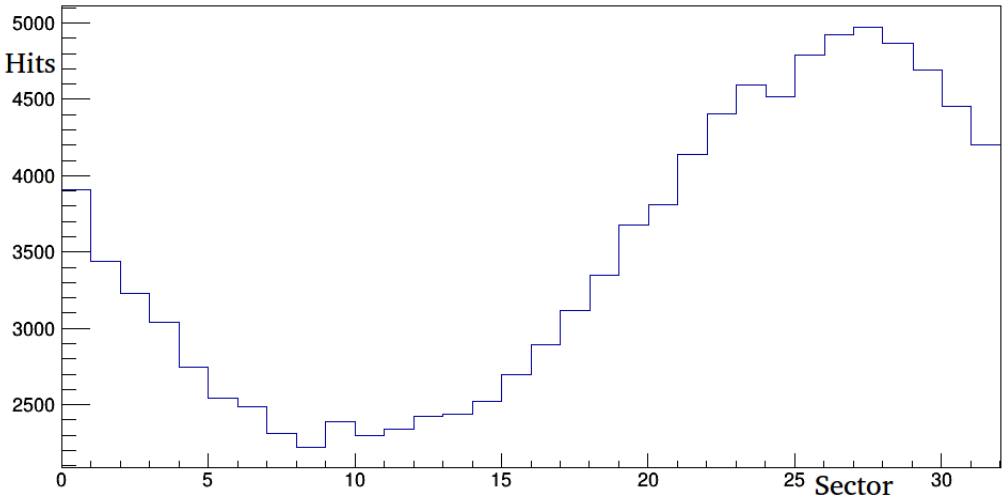

Figure 10: The hit pattern from the Sd1 detector for the same data set as figure 7. This figure has accounted for all the noise and undesired reactions leaving only the Ag(^{11}Li,^{11}Li)Ag reaction.

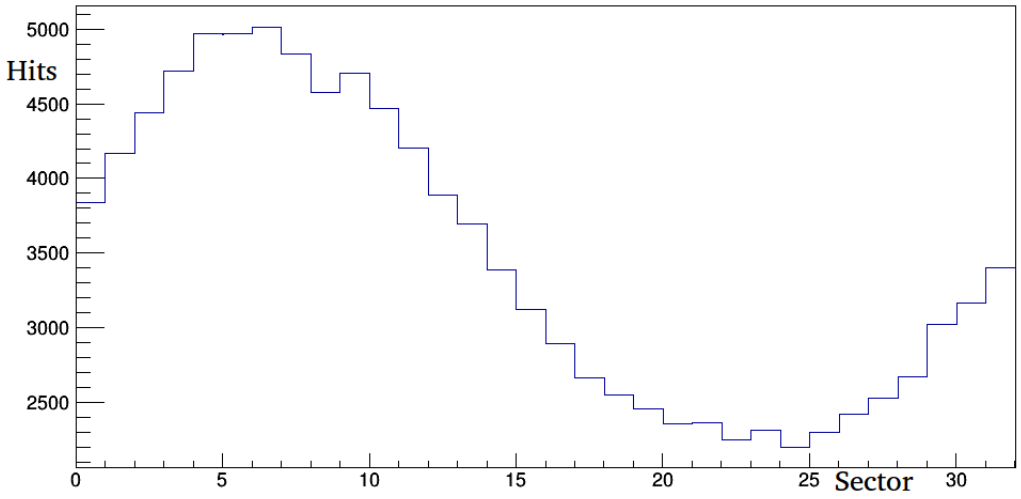

Figure 11: The hit pattern from the Sd2 detector for the same run as figure 10. This is included to show the inverse in hit patterns as mentioned in section 2.2.

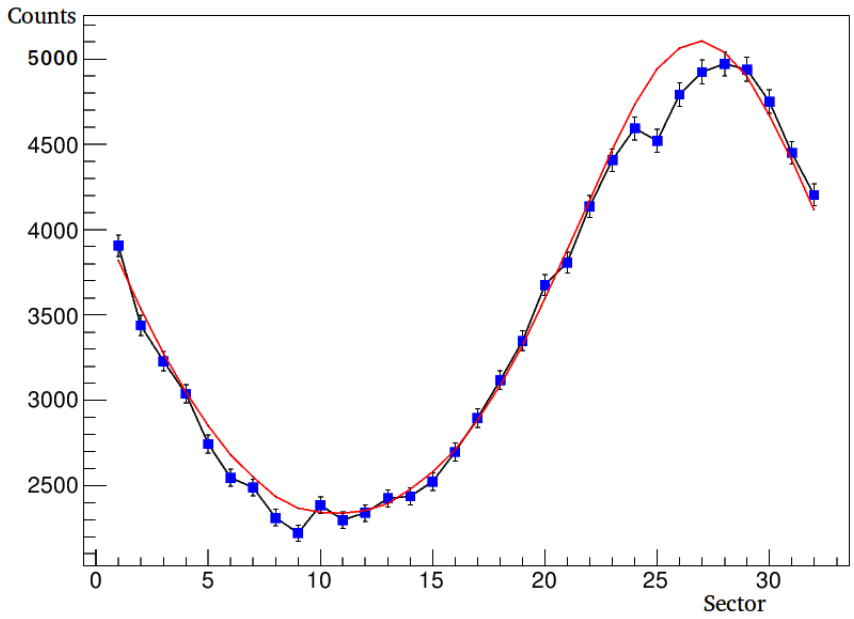

Figure 12: The blue points are the hit pattern the data presented in figure 10. The red curve shows the the simulated hit pattern. The values for the horizontal and vertical shift are 1.33 millimetres and -0.67 millimetres respectively.

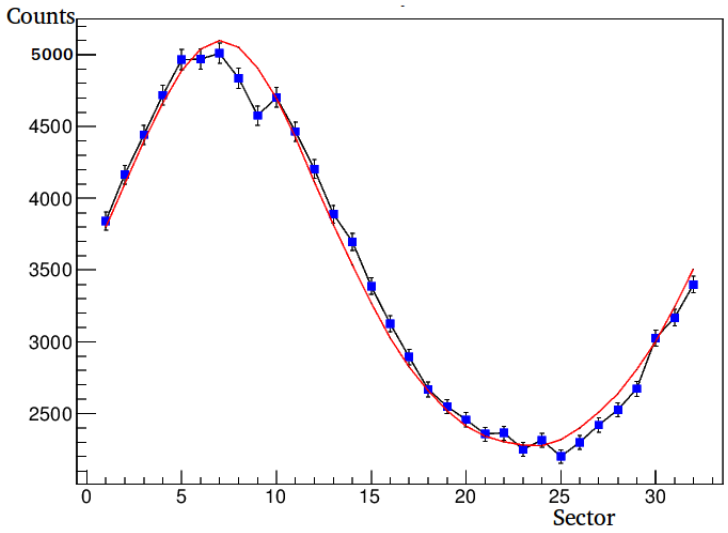

Figure 13: The blue points are the hit pattern the data presented in figure 11. The red curve shows the the simulated hit pattern. The values for the horizontal and vertical shift are 1.47 millimetres and -0.43 millimetres respectively.

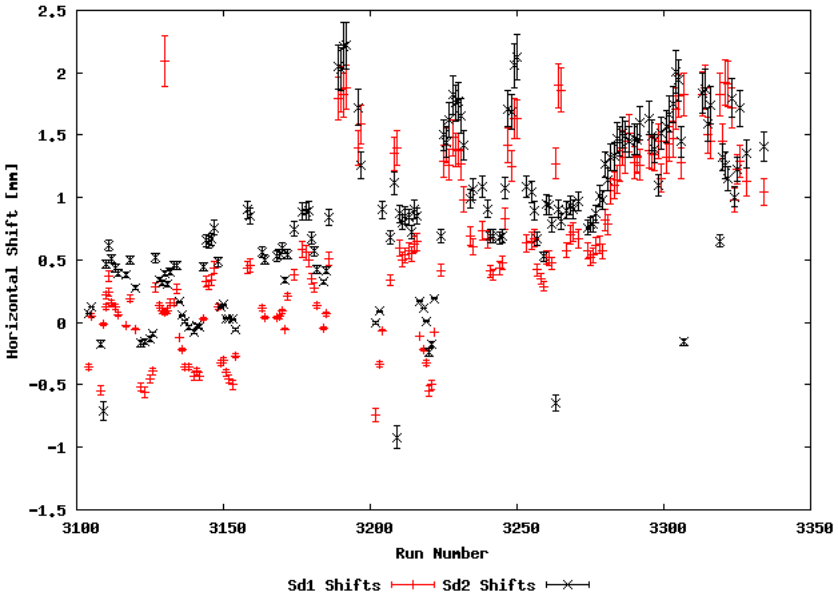

Figure 14: Horizontal shifts over the course of the experiment for both the Sd1 and Sd2 detectors. The vertical axis is shift in millimeters were the horizontal axis is the run number.

In reality, there is no way to tell if the beam is actually shifted or not from this data. It could be shifted, angled, or a combination of the two. The case of no angle and all shift was examined to now and the case of mixing the two scenarios cannot be done with the obtained

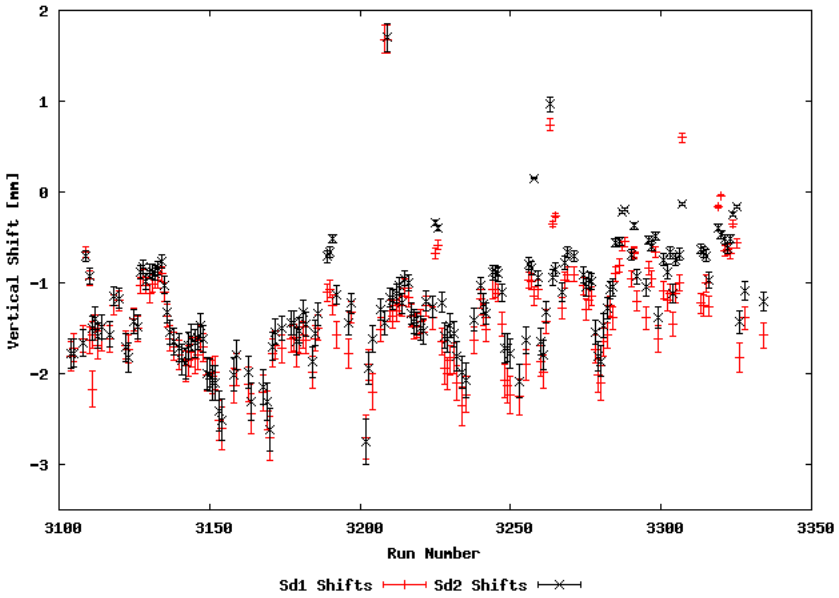

Figure 15: Vertical shifts over the course of the experiment for both the Sd1 and Sd2 detectors. The vertical axis is shift in millimeters were the horizontal axis is the run number.

data. The scenario where the hit pattern is entirely due to angle was then examined using the same Monte Carlo method as described previously. The data is expressed in figures 16 for the changes in polar angle over run number.

3.2 YY1 Shifts

A similar process was done for determining the shifts using the ^{11}Li(p,p)^{11}Li data from the YY1 detector. The issue with the YY1 detector however, is that there is a heat shield that guards a large portion of the detector. The effects of this can be seen in figure 17. This issue combined with the smaller cross-section of the ^{11}Li(p,p)^{11}Li reaction results in significantly less statistics when compared to the Ag(^{11}Li,^{11}Li)Ag reaction for the S3 detectors.

The shield covers a large section of the detector which means only the small angles can be used for calculations. This significantly reduces the statistics in the YY1 measurements and

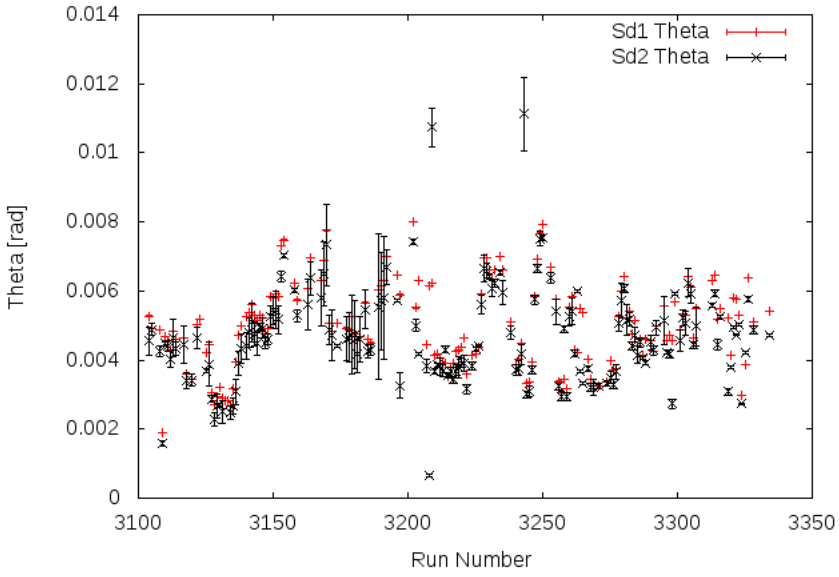

Figure 16: The angle theta over the course of the experiment using data from both the Sd1 and Sd2 detectors. The vertical axis is angle in radians and the horizontal axis is run number.

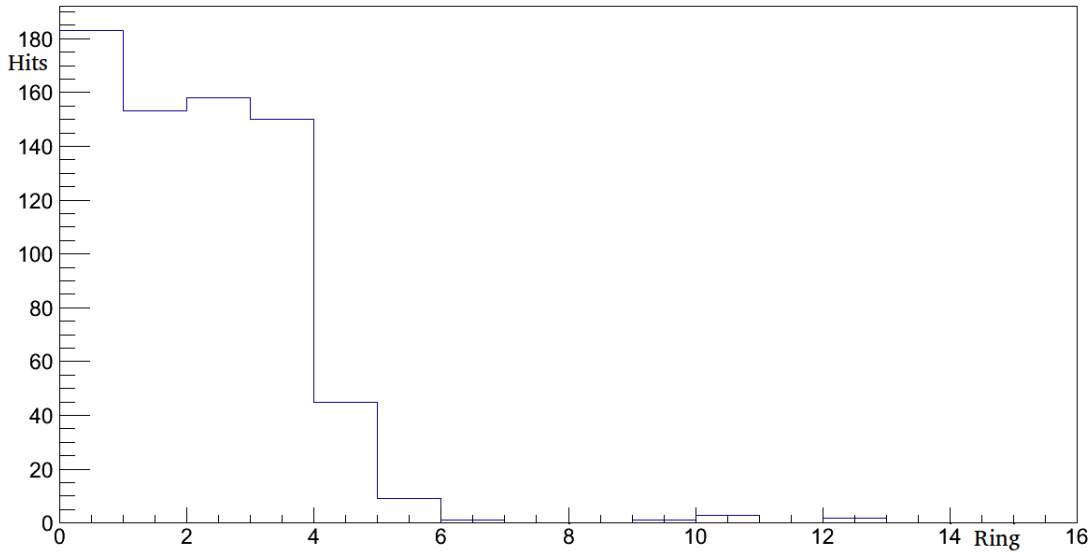

Figure 17: The effect of the heat shield on the theta hit pattern of the YY1 detector. The larger the ring number (horizontal axis) the higher the scattering of the particle.

because of this, 20 runs were combined into one file for better statistics. These small statistics lead to a significant uncertainty in the shift calculations and hit patterns alike (figures

18, 19 and 20). To account for this, twenty runs (each run is $\sim$ two hours) were combined and analysed in chunks at a time as opposed to individually.

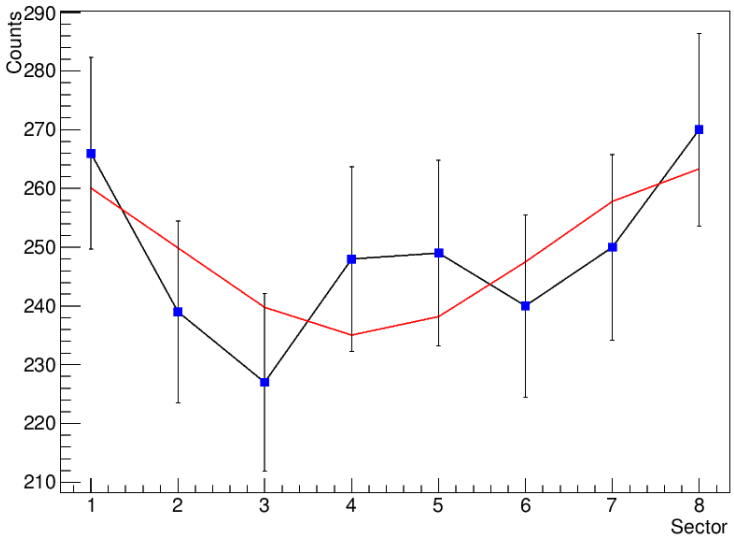

Figure 18: A sample fitted hit pattern from one of the sections of twenty runs for the YY1 detector. Horizontal and vertical shifts were calculated to be -0.21 millimetres and 0.07 millimeters repectively.

There is a clear change in each of the vertical shifts calculated with the data from the YY1 detector. This is potentially caused by a lack of statistics in the data. Because of this variance and uncertainty, the fit was not done using beam angle as it would be just as variant.

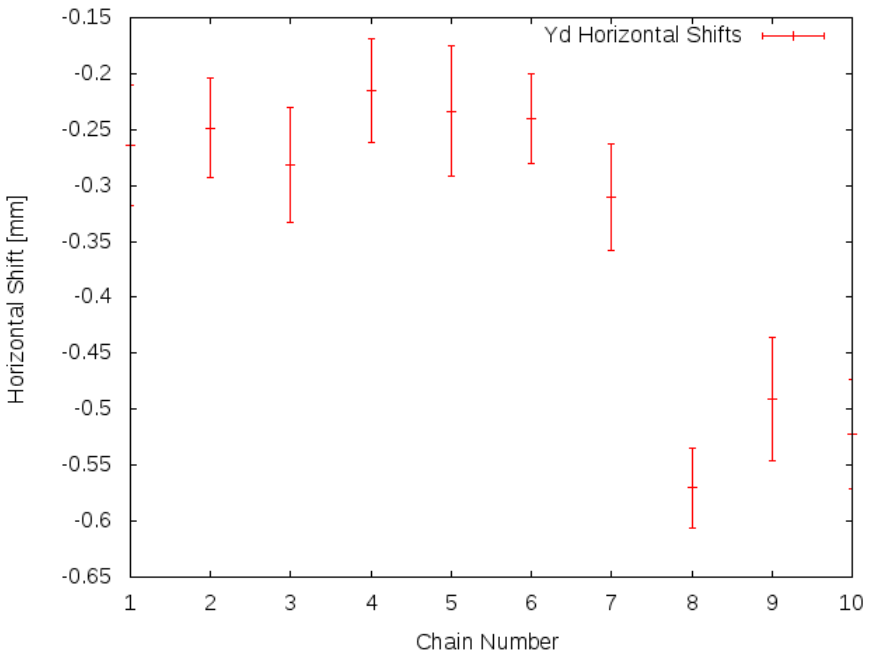

Figure 19: The progression of horizontal shifts relative to the YY1 detector over the course of the experiment. The horizontal axis shows which segment (chain) of twenty (1-10 where 10 has seventeen runs) where the vertical axis shows the shift in millimeters.

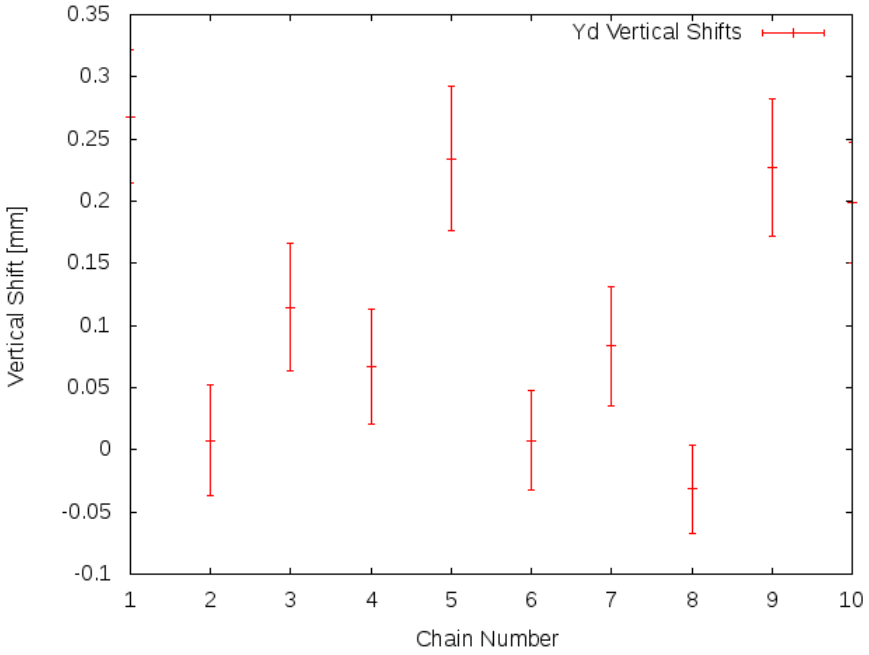

Figure 20: The progression of vertical shifts relative to the YY1 detector over the course of the experiment. The horizontal axis shows which segment (chain) of twenty (1-10 where 10 has seventeen runs) where the vertical axis shows the shift in millimeters.

4 Conclusion

The data reported in this thesis was acquired in Vancouver, Canada at the TRIUMF facility from the experiment with a ^{11}Li beam [3]. Using the IRIS facility, the halo nucleus of ^{11}Li was explored. The present analysis suggests that the shift in the beam was dynamic throughout the experiment. Even though the beam was focussed within two-millimetres of the target cell, the beam could still be shifted up to two millimetres. This much shift would result in an energy-loss difference of anywhere between 0.5% to 1% for the S3 detectors. In the case of the ^{11}Li experiment, this translates to approximately 50keV to 100keV in energy difference between the non-shifted case and the maximum shifted case.

The large shift as derived from the S3 detector data is an order of magnitude larger than those from the YY1 detector. This suggests that the beam position might not be shifted but the beam angle could be the reason for the azimuthal asymmetry. A shift of two-millimetres as calculated seems too large since the beam tuning was done using a two-millimetre collimator (placed at the center of the beam line). The target cell itself is five-millimetres in diameter therefore a beam shift of two-millimetres in one direction would lead to the beam being dominantly outside the target. This seems unrealistic from the measured spectra so the asymmetrical distribution in phi is likely due to a combination of beam angle and shift.

References

[1] Curie, I., Juliot-Curie, F., R. Acad. Sci. 198, 254 1934

[2] Curie, M., Radium and the New Concepts in Chemistry, Nobel Lecture, 1911

[3] Habashi, F., Niepce de Saint-Victor and the Discovery of Radioactivity, Bull. Hist. Chem., 26-2, 2001

[4] Kanungo, R., et al. S1147 proposed, Investigation of low-lying resonances in ^{11}Li

[5] Rutherford, E., The Scattering of α and β Particles by Matter and the Structure of the Atom, Philosophical Magazine, 6-21-125, pg 669-688, 1911

[6] Tanaka, Junki. 2016

[7] Tanihata, I., Neutron Halo Nuclei, J. Phys. G: Nucl. Part. Phys. 22, 1996 157–198.